Circulation Research

ORIGINAL RESEARCH

Tropoelastin Improves Post-Infarct Cardiac Function

Robert D. Hume, Shaan Kanagalingam, Tejas Deshmukh, Siqi Chen, Suzanne M. Mithieux, Fairooj N. Rashid, Iman Roohani, Juntang Lu, Tram Doan, Dinny Graham, Zoe E. Clayton, Eugene Slaughter, Eddy Kizana, April S. Stempien-Otero, Paula Brown, Liza Thomas, Anthony S. Weiss, James J.H. Chong

BACKGROUND: Myocardial infarction (MI) is among the leading causes of death worldwide. Following MI, necrotic cardiomyocytes are replaced by a stiff collagen-rich scar. Compared to collagen, the extracellular matrix protein elastin has high elasticity and may have more favorable properties within the cardiac scar. We sought to improve post-MI healing by introducing tropoelastin, the soluble subunit of elastin, to alter scar mechanics early after MI.

METHODS AND RESULTS: We developed an ultrasound-guided direct intramyocardial injection method to administer tropoelastin directly into the left ventricular anterior wall of rats subjected to induced MI. Experimental groups included shams and infarcted rats injected with either PBS vehicle control or tropoelastin. Compared to vehicle treated controls, echocardiography assessments showed tropoelastin significantly improved left ventricular ejection fraction (64.7±4.4% versus 46.0±3.1% control) and reduced left ventricular dyssynchrony (11.4±3.5 ms versus 31.1±5.8 ms control) 28 days post-MI. Additionally, tropoelastin reduced post-MI scar size (8.9±1.5% versus 20.9±2.7% control) and increased scar elastin (22±5.8% versus 6.2±1.5% control) as determined by histological assessments. RNA sequencing (RNAseq) analyses of rat infarcts showed that tropoelastin injection increased genes associated with elastic fiber formation 7 days post-MI and reduced genes associated with immune response 11 days post-MI. To show translational relevance, we performed immunohistochemical analyses on human ischemic heart disease cardiac samples and showed an increase in tropoelastin within fibrotic areas. Using RNA-seq we also demonstrated the tropoelastin gene *ELN* is upregulated in human ischemic heart disease and during human cardiac fibroblast-myofibroblast differentiation. Furthermore, we showed by immunocytochemistry that human cardiac fibroblast synthesize increased elastin in direct response to tropoelastin treatment.

CONCLUSIONS: We demonstrate for the first time that purified human tropoelastin can significantly repair the infarcted heart in a rodent model of MI and that human cardiac fibroblast synthesize elastin. Since human cardiac fibroblasts are primarily responsible for post-MI scar synthesis, our findings suggest exciting future clinical translation options designed to therapeutically manipulate this synthesis.

GRAPHIC ABSTRACT: A graphic abstract is available for this article.

Key Words: collagen ■ echocardiography ■ elastin ■ heart ■ myocardial infarction ■ therapeutics ■ tropoelastin

Meet the First Author, see p 5

Heart disease is the single largest cause of death worldwide.[1] A prominent subcategory within this range of diseases is ischemic heart disease with myocardial infarction (MI) and subsequent heart failure associated with high morbidity and mortality.[1] In the first few days post-MI, the immune system removes necrotic cells and extracellular matrix (ECM) through complex enzymatic degradation processes.[2] Approximately 3 days post-MI, fibroblast proliferation and replacement fibrosis begins, with the formation of a collagen I-rich scar.[2] Unlike healthy myocardium, the fibrotic scar is electrically inert, less contractile, and has an increased stiffness, with the ensuing heart failure causing potential morbidity and mortality. The increased intracardiac wall stiffness is

Correspondence to: James J.H. Chong, PhD, Center for Heart Research, Westmead Institute for Medical Research, Westmead NSW 2145, Australia. Email james.chong@sydney.edu.au

Supplemental Material is available at https://www.ahajournals.org/doi/suppl/10.1161/CIRCRESAHA.122.321123.

For Sources of Funding and Disclosures, see page 84.

Novelty and Significance

What Is known?

- Direct myocardial injections in small animal models require complex, slow, invasive thoracotomy surgery.
- Tropoelastin improves dermal wound healing in both small and large animal models.
- Cell-delivered rat elastin improves rat heart function postmyocardial infarction by reducing scar expansion.

What New Information Does This Article Contribute?

- Ultrasound-guided closed chest direct myocardial injections provides a new faster, safer, and less invasive protocol for therapeutic testing in rats.
- Human tropoelastin improves rat heart function post-myocardial infarction and could potentially be used to treat heart failure.
- Elastogenesis occurs during replacement fibrosis in human heart disease and can be accelerated in vitro via tropoelastin treatment.

Tropoelastin is a highly elastic natural biomaterial that despite encouraging findings in dermal wound healing, has not yet been significantly investigated in cardiac repair. We developed a novel ultrasound-guided intramyocardial injection protocol that circumvents the need for thoracotomy in rats already subjected to myocardial infarction (MI). Using this protocol, we injected purified human tropoelastin directly into the left ventricular myocardium and show improvement in heart function post-MI. We further elucidate the underlying mechanisms resulting in improved systolic function using echocardiographic strain analysis. Although tropoelastin expression is thought to be restricted to embryonic/neonatal development, our novel findings show tropoelastin gene and protein expression is upregulated in adult human cardiac disease and fibrosis. We also identify the human cardiac fibroblast (cFib) as the potential source of underappreciated cardiac injury-induced elastogenesis. Finally, we demonstrate that manipulation of cFib elastogenesis can be achieved by addition of exogenous tropoelastin. This provides evidence for potential clinical translation of tropoelastin to treat and improve the lives of the millions of heart failure patients worldwide.

Nonstandard Abbreviations and Acronyms

cFib	human cardiac fibroblasts
DE	differential gene expression
ECM	extracellular matrix
IZ	infarct zone
LV	left ventricle
LVAW	left ventricular anterior wall
LVEF	left ventricular ejection fraction
MI	myocardial infarction
MI+PBS	myocardial infarction with phosphate buffered saline vehicle control injection group
MI+Tropo	myocardial infarction with tropoelastin injection group
RNAseq	RNA sequencing

largely due to the deposition of collagen I.[3,4] This resultant mechanical mismatch of the post-MI scar and healthy myocardium causes abnormally amplified region-specific stresses, accompanied by varied systolic and diastolic functional outcomes.[5–7] After initial replacement fibrosis, scar expansion caused by increased wall stresses exacerbates adverse cardiac remodeling, resulting in an increased prevalence of heart failure and death.[8,9]

Tropoelastin is a highly elastic molecule with an exceptionally low elastic modulus of ~3 kPa.[10,11] It is also the soluble monomer subunit of the highly elastic ECM protein elastin, which is the major component of all elastic fibers within the body.[11] Elastin has a stiffness modulus of ~1 MPa which, although an order of magnitude higher than tropoelastin, is substantially lower than other ECM proteins, for example, collagen ranges 160 to 7500 MPa.[11,12] Elastin is integral in allowing continuous stretch and recoil events without causing permanent deformation in a range of elastic tissues, including within the cardiovascular system.[11,13]

Synthesis of tropoelastin and elastin fibers (elastogenesis) is restricted to the developing fetus and during infancy.[11,14] However, some studies have shown elastin synthesis during adulthood in response to injury, disease, and after MI.[15–19] Importantly, the application of tropoelastin in both small and large animal models of dermal injury has shown therapeutic benefit by improving the wound healing response.[20,21] Using cell therapy techniques, others have shown rat elastin fragment delivery in a rat model of MI can improve cardiac functional outcomes.[22,23] However, the effects of purified human tropoelastin post-MI without confounding cellular components remains unclear.

Previous studies have shown that injections of ECM components into the left ventricular (LV) wall after MI can improve LV scar mechanics and heart function.[24–27] We

therefore hypothesized that therapeutic delivery of purified human tropoelastin into the healing LV wall would decrease subsequent LV stiffness and adverse remodeling. Here, we show that purified human tropoelastin decreases scar expansion, increases scar elastogenesis, improves LV systolic contraction, and reduces gene expression of immune response pathways in a rat model of subacute MI. Highlighting translational significance, we also demonstrate that the tropoelastin gene (*ELN*) and its related protein is expressed in human ischemic heart disease cardiac samples. Furthermore, we demonstrate that the key drivers of the post-MI scar, human cardiac fibroblasts (cFib), have propensity to upregulate *ELN* during myofibroblast differentiation and increase elastogenesis in response to tropoelastin treatment. Therefore, our study establishes purified human tropoelastin as a novel therapy to treat post-MI healing.

METHODS

Data Availability

The data that support the findings of this study are available from the corresponding author upon reasonable request. For a detailed description of all methods and materials used, please refer to the Supplemental Methods and Major Resources Table in the Supplemental Materials.

Sprague–Dawley rats were subjected to MI by left anterior descending coronary artery ligation and then randomized to (1) sham operated, (2) noninfarcted tropoelastin injected (Tropo), (3) infarcted vehicle control injected (MI+PBS), and (4) infarcted tropoelastin injected groups (MI+Tropo). Tropoeleastin was injected into the healing LV wall 4 days post-MI under ultrasound-guidance. High-frequency echocardiography was performed at baseline before MI (day −1), pretreatment post-MI (day 3), and posttreatment (days 14 and 28) before rats were euthanized (day 28) and hearts collected. Echocardiographic, cellular, and molecular analyses were performed blinded to treatment group.

RESULTS

Ultrasound-Guided Injections Allow Intramyocardial Delivery of Tropoelastin

Thoracotomy is often used in translational studies to enable delivery of investigational therapeutic agents. This approach is difficult and carries significant animal morbidity and mortality. To circumvent these potential complications, we developed an ultrasound-guided method to inject directly into the myocardium of the left ventricle (LV; Figure 1). Our protocol required the ultrasound probe to be prealigned with a 1.5″ hypodermic needle and syringe in a purpose specific holder (Figure 1A). As a pilot to visualize our injection site, healthy rats were injected with Alcian blue dye, with necropsy showing no evidence of punctured lungs or any other organ damage at the injection site (Figure 1B) and successful intramyocardial injection into the left ventricular anterior wall (LVAW; Figure 1B through 1D). For post-MI tropoelastin injections, we used a short axis view to approach the LVAW at a 45° angle with the needle bevel downwards (Figure 1E; Video S1 through S4). Successful injection was indicated by a change in brightness within the wall and after removal of the needle (blue arrow, Figure 1E; Video S1 through S4). Using our protocol, no rats showed any signs of pain or distress following recovery from anesthesia and during the 24-day follow-up (data not shown). All rats that survived MI surgery and received injections survived the entire study (100%, 28 days).

Tropoelastin Improves Cardiac Function Post-MI by Increasing LV Systolic Contractility

The number of neutrophils that synthesize elastases peaks within the first 0 to 3 days following MI.[2,28,29] At this timepoint, both fibroblast proliferation and replacement fibrosis increases.[2] We therefore chose to inject tropoelastin 4 days post-MI to avoid elastase degradation and to encourage elastogenesis by proliferating fibroblasts (Figure 2A). This also enabled us to measure cardiac function (operator blinded to treatment group) at baseline (day −1), post-MI pretreatment (day 3), and 2 post-MI posttreatment (day 14 and day 28) timepoints (Figure 2A). To determine an efficacious dosage of tropoelastin, we ran a pilot study using both 1 mg/mL and 10 mg/mL concentrations. Although 10 mg/mL produced an early improvement in left ventricular ejection fraction (LVEF) at day 14, by day 28 it had deleterious effects on cardiac function (Figure S1A). Additionally, large but thin-walled blood vessels were seen in the infarcted region of 10 mg/mL tropoelastin treated rats suggesting suboptimal angiogenesis had occurred (Figure S1B). For these reasons, the lower dose of 1 mg/mL was selected for use in the rest of the study.

Short axis M-mode ultrasound measurements of LV function using the Teicholz method (Figure 2B through 2F) demonstrated an expected decline in heart function 3 days post-MI (Figure 2B through 2D) with no significant differences in heart rate at the time of measurement (Figure S2). Healthy (noninfarcted) rats injected with tropoelastin showed no effects in heart function over 28 days (denoted Tropo; Figure 2), demonstrating that the protein had no deleterious effects in a noninfarct setting. At the day 14 post-MI timepoint, infarcted tropoelastin-treated rats (MI+Tropo) showed a trend of improved LVEF and fractional shortening (Figure 2B through 2D; Figure S3). By 28 days, MI+Tropo rats demonstrated significantly improved fractional shortening and LVEF (64.7±4.4% versus 46.0±3.1% control; Figure 2B through 2D). Interestingly, this improvement was driven by a decreased LV systolic diameter (Figure 2E; Figure S4A) and increased LVAW systolic thickness (Figure 2F; Figures S4B and S5), with no significant differences to LV diastolic diameter or left ventricular posterior wall thickness

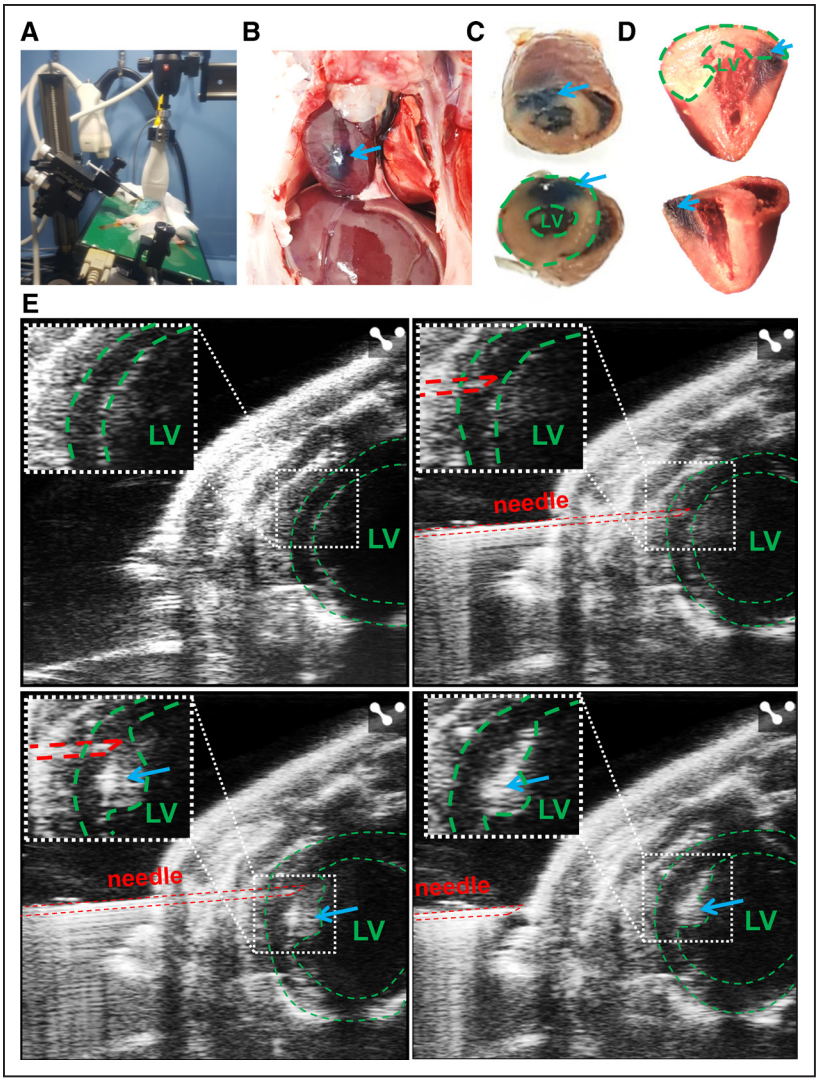

Figure 1. Ultrasound-guided injections permit a less invasive intramyocardial therapeutic delivery of tropoelastin. **A**, Photographs of rat position, stage, syringe, and ultrasound probe setup for ultrasound-guided intramyocardial injections. **B**, Photograph of rat dissection immediately following Alcian blue (blue arrow) intramyocardial injection. **C**, Photograph of Alcian blue (blue arrows) injected-rat heart. **Left**: basal half. **Right**: apical half. **D**, Stereoscopic image of a mid-to-apex rat heart injected with Alcian blue (black arrows). **Left/right**: left/right half of the left ventricle (LV). **E**, Short axis echocardiograms showing intramyocardial delivery of tropoelastin. **Top left** (preinjection): view of the LV wall (green dotted line) with an enhanced image of the left ventricular anterior wall ([LVAW], white dotted box and enhanced insert). **Top right** (preinjection): needle (red dotted line) shown within the LVAW. **Bottom left** (mid-injection): injection of tropoelastin (blue arrow) into the LVAW. **Bottom right** (postinjection): needle removed from the skin with tropoelastin (blue arrow) remaining in the LVAW.

(Figure S4C through S4J and S5). To confirm our short axis results, we performed separate analyses of parasternal long axis B-mode measurements (Video S5 through S16) by 2 blinded observers. These results also showed no statistically significant change in heart rate between groups at the time of measurement and showed tropoelastin improved LVEF and fractional shortening post-MI (Figure S6). Both intra and interobserver measurements showed low levels of bias and tight levels of agreement at all timepoints (Figure S7). Together, our data show that tropoelastin improves post-MI LVEF through increased systolic contraction and increased LVAW thickness. Notably, the LVAW was the location of tropoelastin injections.

Tropoelastin Improves LVAW Strain and Reduces LV Dyssynchrony

LV strain is an important echocardiography parameter that evaluates myocardial deformation. It is a surrogate for LV contraction function and utilized to measure function of cardiac tissue.[30] Global longitudinal strain measures the LV ability to contract in the longitudinal direction, with a lower negative value suggestive of adverse remodeling.[30] We showed that post-MI tropoelastin improved global longitudinal strain compared to MI+PBS controls (Figure 3A through 3C) and therefore increased overall cardiac contraction in the longitudinal direction.

Segmental strain analyses allow measurements of specific LV regions and their mechanics.[31] LV radial strain is also a measurement of myocardial deformation, with a decrease below baseline indicative of cardiac dysfunction. Segmental analyses showed post-MI tropoelastin treatment significantly increased (improved) radial strain in LVAW base and LVAW mid segments with no significant effects strain in any other segment, as compared to MI+PBS controls at day 28 (Figure 3D through 3F and 3H through 3K; Figures S8 and S9). Post-MI tropoelastin also significantly decreased (improved) longitudinal strain in LVAW apex segments with no significant effects in any other segment (Figure 3D, 3G, 3L, and 3M; Figures S8 and S9). No significant effects of post-MI tropoelastin were observed in the left ventricular posterior wall (Figure S9). Thus, all significant functional strain improvements were restricted to the LVAW, the location

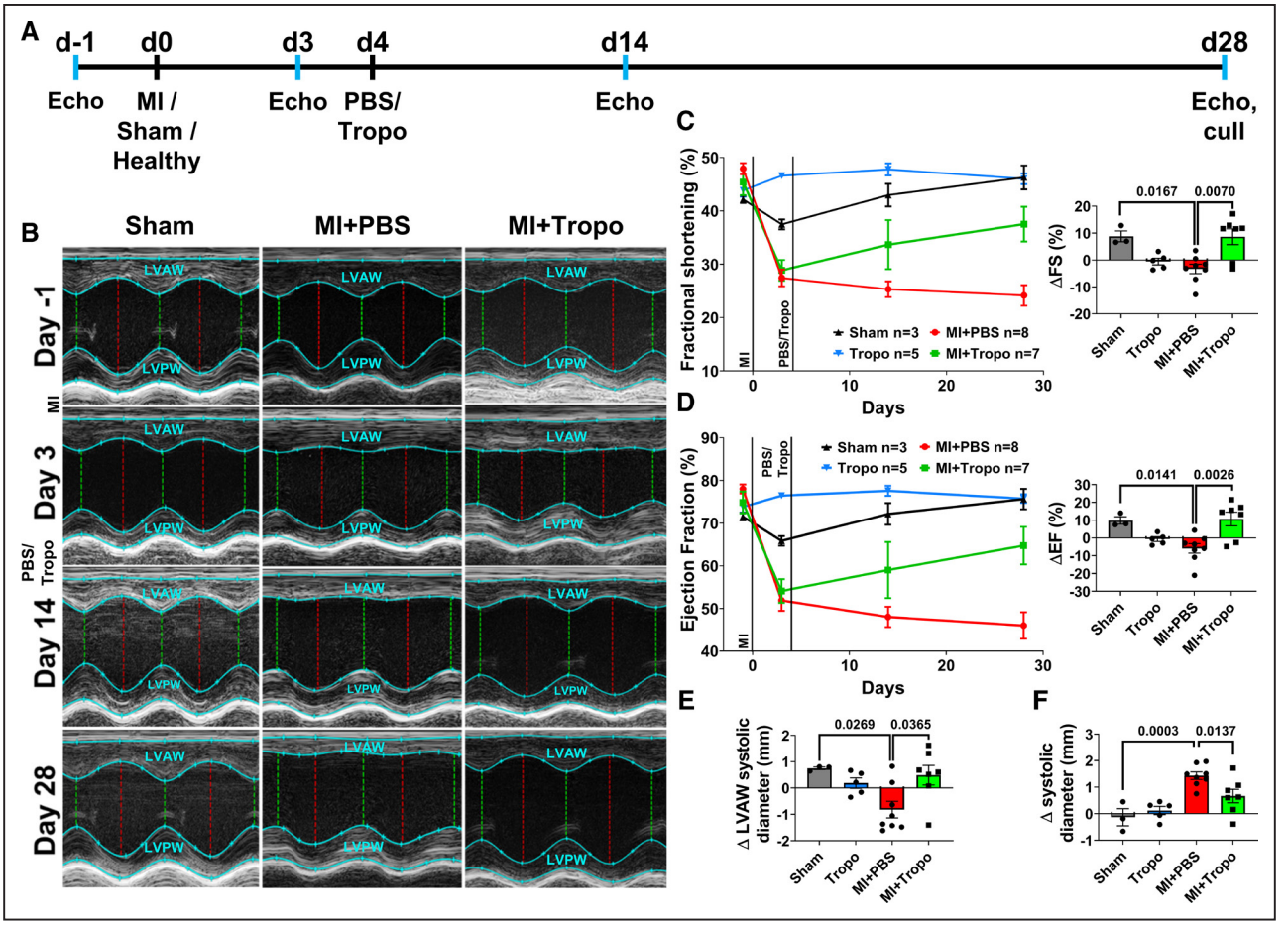

Figure 2. Tropoelastin improves heart function post-myocardial infarction (MI).
Rats underwent MI, sham surgery, or no surgery (Healthy), echocardiography (echo), and intramyocardial injection of tropoelastin (Tropo) or phosphate buffered saline (PBS) vehicle control. **A**, Experimental timeline. **B**, Representative left ventricle short axis (LVSAX) mid-papillary M-mode echocardiographic images. **C** and **D**, LVSAX M-mode analyses for fractional shortening (FS) and ejection fraction (EF) over time and for the change (Δ) from day 3 to day 28 post-MI. **E** and **F**, LVSAX M-mode analyses for the change (Δ) from day 3 to day 28 post-MI in LV systolic diameter (**E**) and left ventricular anterior wall (LVAW) systolic diameter (**F**). Statistical analyses: Conover-Iman multiple comparison test with Holm-Bonferroni correction. Exact *P*-values are represented above graphs to 4 decimal points.

of both the infarct and the intramyocardial tropoelastin injections.

Within the uninjured LV, it is essential that opposing walls (eg, LVAW and left ventricular posterior wall) contract in synchrony to ensure efficient LV contraction (Figure S10).[32] Conversely, intraventricular dyssynchrony is associated with pathological conditions such as MI.[32,33] We utilized 2D speckle tracking echocardiography to evaluate dyssynchrony by measurement of the time-to-peak systolic strain from the parasternal long axis images. We then compared the time-to-peak of opposing wall segments (Figure S10) and assessed the maximum opposing wall delay; a measurement of LV dyssynchrony. This showed that tropoelastin significantly reduced the maximum opposing wall delay in infarcted rats and thus reduced dyssynchrony for radial velocity, displacement, strain and strain rate, when compared to control rats (Figure 3N through 3Q; Figure S11). Therefore, our data show that tropoelastin also improves post-MI function by decreasing intraventricular dyssynchrony.

Tropoelastin Reduces Scar Size and Increases Scar Elastogenesis

Increased post-MI scar size is correlated with decreased heart function.[34] We therefore quantified collagen in post-MI hearts using Picrosirius red histological staining and showed that tropoelastin significantly reduced scar size (8.9±1.5% MI+Tropo versus 20.9±2.7% MI+PBS control; Figure 4A through 4C). Healthy rats injected with tropoelastin (denoted as Tropo) showed no statistically significant increase in fibrosis compared to sham controls, demonstrating that in the healthy cardiac setting tropoelastin does not induce fibrosis (Figure 4C). These results suggest post-MI tropoelastin treatment improves heart function by reducing scar expansion.

Tropoelastin that is synthesized in vivo is organized and cross-linked into insoluble elastin via elastogenesis.[11] To determine whether intramyocardial injection of tropoelastin resulted in elastogenesis and therefore increased elastin fibers, we performed Verhoeff

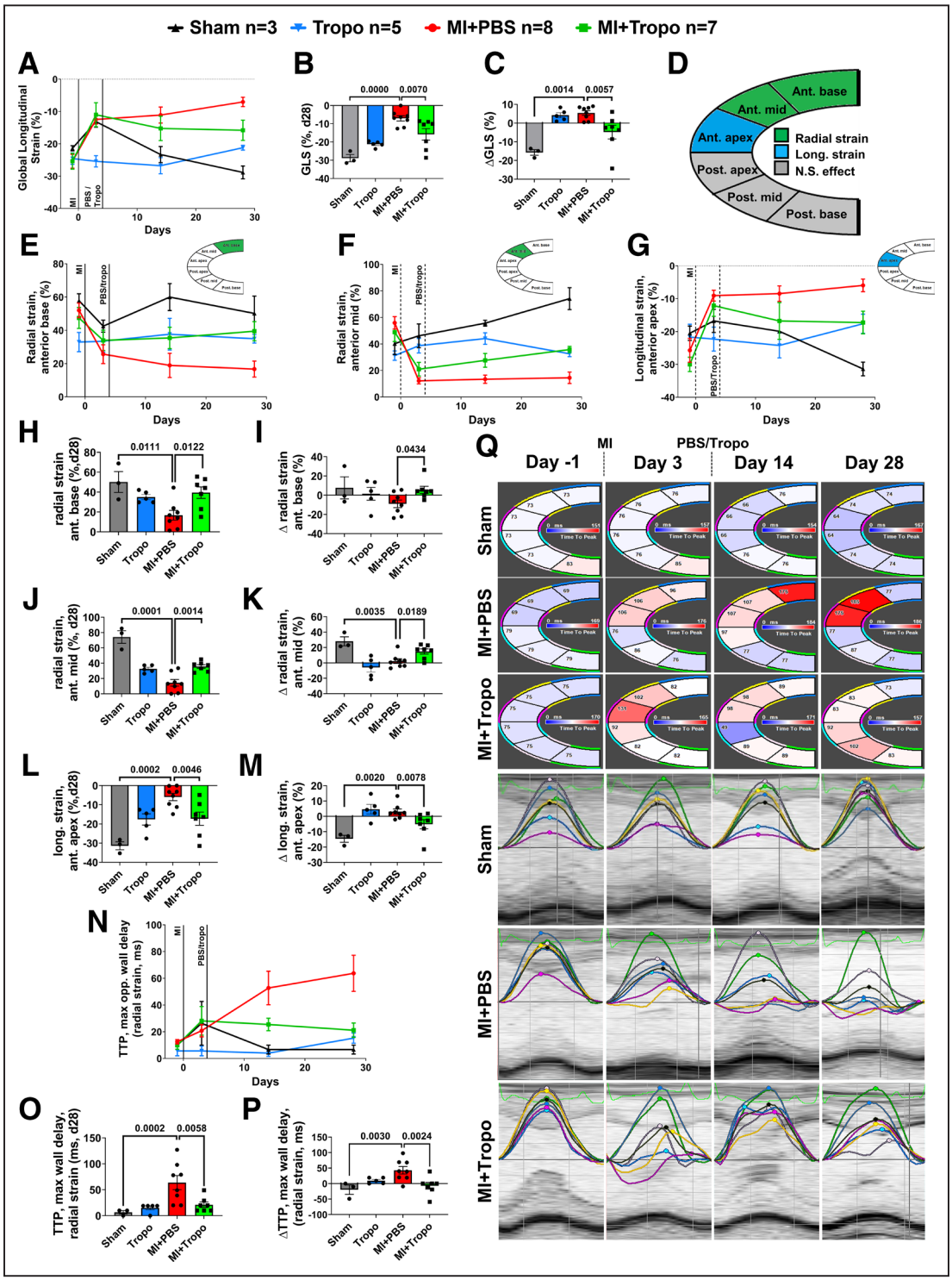

Figure 3. Tropoelastin reduces left ventricle (LV) dyssynchrony and alters LV anterior wall mechanical dispersion.
A–**C**, Speckle tracking analyses of parasternal long axis (PSLAX) B-mode measurements for global longitudinal strain (GLS) over time (**A**), 28 days post-myocardial infarction (MI) (**B**) or the change (Δ) from day 3 to day 28 post-MI. **D**, Schematic of significantly improved segmental strain following tropoelastin treatment in infarcted animals. **E**–**G**, LV anterior wall segmental radial (**E**, **F**) and longitudinal (**G**) strain over time. **H**–**M**, LV anterior wall segmental radial (**H**–**K**) and longitudinal (**L**, **M**) 28 days post-MI (d28) or the change (Δ) from day 3 to day 28 post-MI. **N**–**P**, LV time-to-peak (TTP) analyses for maximum radial strain throughout one cardiac cycle as a measurement of mechanical dyssynchrony over time (n), on day 28 (**O**) or the change (Δ) from day 3 to day 28 (**P**) post-MI. **Q**, LV TTP analyses for maximum radial strain throughout one cardiac cycle. TTP is represented as a blue-red heatmap within each segment (**top**, schematics) or a circle at the peak of each line (**bottom**, graphs). LV base (blue), mid (yellow), and apex (purple) anterior wall segments and LV base (green), mid (grey), and apex (cyan) posterior wall segments are colored around each segment (**top**, schematics) and on each corresponding line (**bottom**, graphs). MI+Tropo rats show reduced dyssynchrony on day 28 vs MI+PBS controls. Statistical analyses: Conover-Iman multiple comparison test with Holm-Bonferroni correction, exact *P*-values represented above graphs to 4 decimal points. MI+PBS indicates myocardial infarction with phosphate buffered saline vehicle control injection group; and MI+Tropo, myocardial infarction with tropoelastin injection group.

ORIGINAL RESEARCH

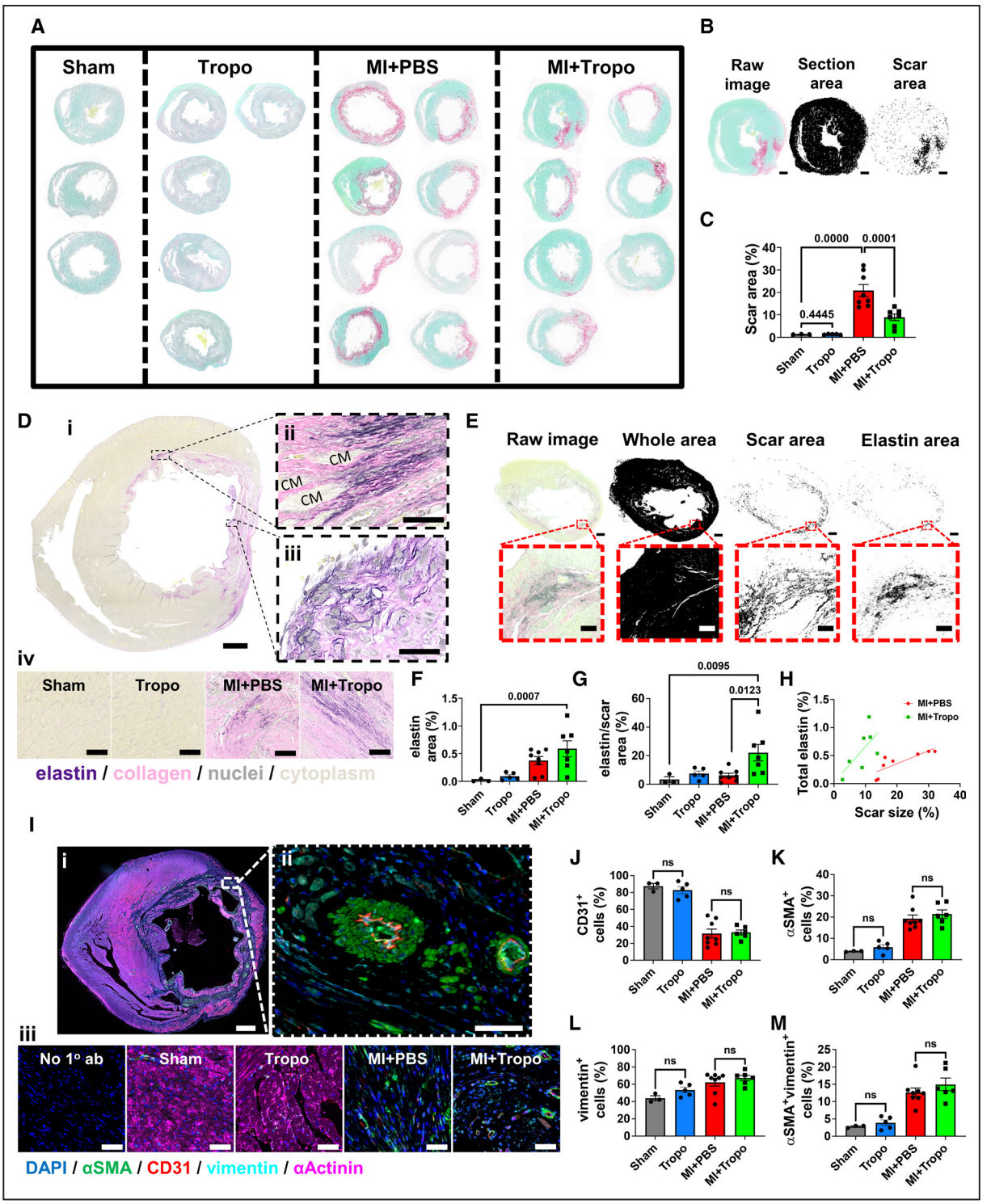

Figure 4. Tropoelastin reduces scar size and increases scar elastogenesis.
A, Picosirius red (PSR) and fast green histological stain showing post-myocardial infarction (MI) scar size (red). **B**, Color thresholding for scar size measurements. Scale bar=1 mm. **C**, Scar area analysis (PSR area/total section area). **D**, Verhoeff van Gieson histological staining showing elastin fibers (dark purple) within the post-MI scar (pink), scale bars 1 mm (i), 50 µm (ii, iii), 100 µm (iv). **E**, Color thresholding for elastin image analysis. **F**, Elastin area analysis (elastin area/total section area). Scale bars=1 mm and 100 µm for magnified inserts. **G**, Elastin scar contribution analysis (elastin area/scar area). **H**, Total elastin (%) vs scar size (%). **I**, Representative immunohistochemical (IHC) images. Scale bars=1 mm (i), 50 µm (ii), 100 µm (iv). **J**–**M**, Cell profiler IHC analyses % of CD31$^+$, α-smooth muscle actin$^+$ (αSMA$^+$), vimentin$^+$, and αSMA$^+$vimentin$^+$ cells within infarct scars. All images shown are transverse cut cardiac sections of both the left and right ventricles. Statistical analyses: Conover-Iman multiple comparison test with Holm-Bonferroni correction, exact *P*-values represented above graphs to 4 decimal points. CM indicates cardiomyocytes; DAPI, 4′,6-diamidino-2-phenylindole; No 1° ab, no primary antibody control; MI+PBS, myocardial infarction with phosphate buffered saline vehicle control injection group; and MI+Tropo, myocardial infarction with tropoelastin injection group.

van Gieson histological staining enabling visualization of elastin fibers within the post-MI scar (Figure 4D). Fibrillar elastin was seen within post-MI scars aligned with collagen fibers or around scar-resident cells (Figure 4D). Healthy (noninfarcted) tropoelastin injected rats (denoted Tropo) showed no statistical difference in elastin content compared to shams (Figure 4D through 4F), showing that infarction is required for substantial elastogenesis. In contrast, elastin was significantly increased in tropoelastin-treated infarcted rats (MI+Tropo) compared to both sham and Tropo groups (Figure 4D through 4F). However, elastogenesis in the scar was also seen in MI+PBS control rats (Figure 4F), demonstrating an underappreciated innate ability for elastogenesis in the post-MI scar. As tropoelastin was injected into infarcted myocardium, elastogenesis was restricted to the scar and since it reduced scar size, we next quantified elastin as a proportion of total scar. These results show significantly greater scar elastogenesis after tropoelastin delivery (22±5.8% MI+Tropo versus 6.2±1.5% MI+PBS control; Figure 4G). Additionally, when comparing total elastin to scar size (Figure 4H), we show that MI+Tropo rats have smaller scars with higher overall elastin content.

To analyze the extent to which tropoelastin altered cell composition of the scar, we performed immunohistochemical image analysis using 4 major cell markers (Figure 4I). These markers were α-smooth muscle actin (αSMA) for myofibroblasts/smooth muscle cells, vimentin for fibroblasts, CD31 for endothelial cells, and α-actinin for cardiomyocytes (Figure 4I). Interestingly, no cell type showed significantly different contribution within the healthy LV of Tropo versus sham rats or within the infarct scars of MI+Tropo versus MI+PBS rats (Figure 4I through 4M).

The use of tropoelastin to treat full-thickness skin wounds leads to increased early stage angiogenesis that promotes repair but then is subsequently resolved.[20] To assess whether angiogenesis was detectable in our mature scar, we performed blinded immunohistochemical analyses that showed no significant difference in arteriole or capillary diameter and number (Figure S12, total analyzed: sham 3 animals/30 images/80 vessels, MI+PBS 8 animals/276 images/2412 vessels, MI+Tropo 7 animals/228 images/1868 vessels, technical replicates were averaged to provide 1 measurement/animal). This is consistent with a model where tropoelastin stabilizes the scar by increasing its elastin content and therefore decreasing its stiffness, rather than altering its cellular composition.

To address the hypothesis that tropoelastin decreases scar stiffness, we performed stress-strain mechanical testing on fresh ex vivo LV tissue and assessed infarct zone (IZ) stiffness via elastic modulus (Figure S13A through S13C). For these measurements, a higher elastic modulus signified a stiffer material. We show PBS treatment of infarcts resulted in IZ tissue elastic modulus of 148.5±54.6 kPa, which is 4.7 times higher than healthy LVAW tissue elastic modulus of 31.9±7.6 kPa (Figure S13D). In contrast, treatment of infarcts with tropoelastin resulted in a LVAW IZ elastic modulus of 49.8±12.5 kPa, indistinguishable from both sham (49.0±17.6 kPa) and healthy tissue ($P>0.99$; Figure S13D). There were no statistically significant differences between elastic moduli in remote zone LV tissue (Figure S13E). These data suggest tropoelastin increases infarct elasticity to a value similar to noninfarcted hearts.

Tropoelastin Effects Gene Expression of ECM and Immune-Related Pathways Post-MI

For molecular characterization of the LV during posttreatment scar formation, we collected IZ or remote zone LV tissue for RNA sequencing (RNAseq) at 7 and 11 days post-MI (3 and 7 days posttreatment, respectively; Figure 5A). Differential gene expression (DE) analysis of all groups (IZ, remote zone, day 7, day 11, MI+PBS, MI+Tropo) compared to sham controls revealed DE of 7950 genes in total, with negligible DE genes in remote zone (Figure 5B). This suggests no detectable treatment effects within the post-infarct remote zones and greatest change occurring in the IZ. MI+PBS IZ had greater DE compared to shams (Figure 5B). Reactome pathway analyses comparing DE genes of MI+Tropo IZ versus MI+PBS IZ, showed that MI+Tropo upregulated ECM pathways associated with elastic fiber formation on day 7 but not on day 11 (Figure 5C). This suggests that any increased post-MI elastogenesis after tropoelastin treatment occurs earlier than 11 days post-MI (<7 days posttreatment).

Next, we used the Database for Annotation Visualization and Integrated Discovery to perform gene ontology term analyses, again comparing MI+Tropo IZ to MI+PBS IZ. While no significantly upregulated or downregulated gene ontology terms were identified on day 7, MI+Tropo IZ showed downregulation of multiple immune-related pathways on day 11 (Figure 5D, red asterisks). MI+Tropo IZ also showed multiple downregulated ECM pathways, including some related to collagen fiber formation (Figure 5D, blue asterisks). For upregulated pathways, multiple metabolic and mitochondrial-related gene ontology terms were evident in MI+Tropo IZ tissue (Figure S14). Another pathway named response to xenobiotic stimulus was also upregulated, likely due to the introduction of human tropoelastin into the rat heart (Figure S14). Taken together (with our earlier findings demonstrating that tropoelastin reduces scar expansion) our RNAseq data suggests that therapeutic effects of exogenous tropoelastin delivery begins ≤7 days posttreatment via modulation of immune response and subsequent collagen fiber formation.

ORIGINAL RESEARCH

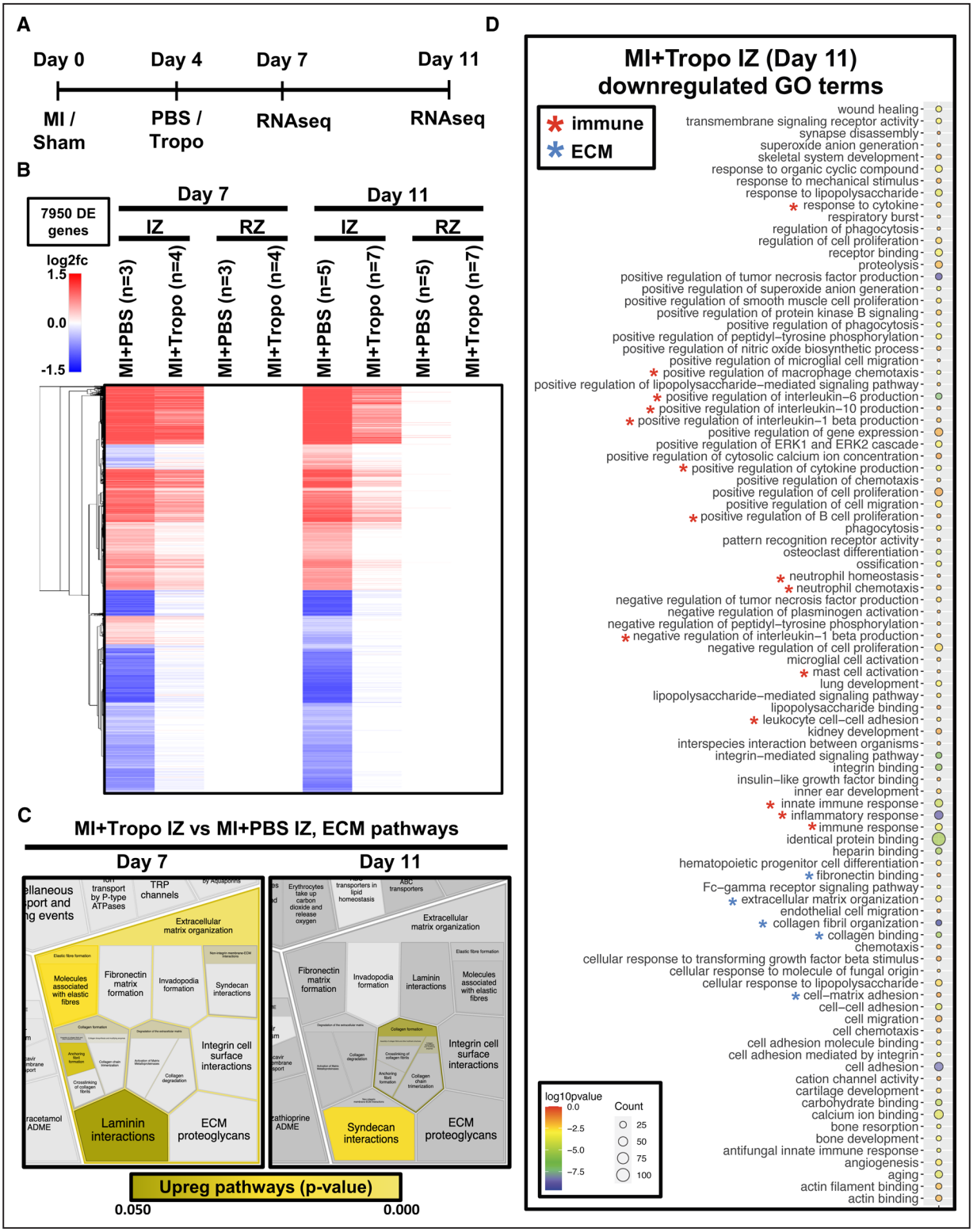

Figure 5. Tropoelastin downregulates gene expression in infarct zone (IZ) immune pathways 11 days post-myocardial infarction (MI). **A**, Schematic of RNA sequencing (RNAseq) experiments. Rats were infarcted (MI), treated with PBS or tropoelastin (Tropo) via ultrasound-guided intracardiac injection, culled, and left ventricle (LV) samples collected for RNAseq. **B**, Heatmap of all IZ and remote zone (RZ) differentially regulated genes in MI+PBS and MI+Tropo rats as compared to Sham LV controls 7 and 12 days post-MI (rats were pooled for analyses). **C**, Reactome analysis of differentially regulated extracellular matrix (ECM) pathways (yellow=significantly upregulated pathways) in MI+Tropo IZ as compared to MI+PBS IZ. **D**, Downregulated gene ontology (GO) terms in MI+Tropo IZ as compared to MI+PBS IZ on day 11 post-MI. Red and blue asterisks represent GO terms associated with immune and ECM pathways, respectively. DE indicates differential gene expression; MI+PBS, myocardial infarction with phosphate buffered saline vehicle control injection group; and MI+Tropo, myocardial infarction with tropoelastin injection group.

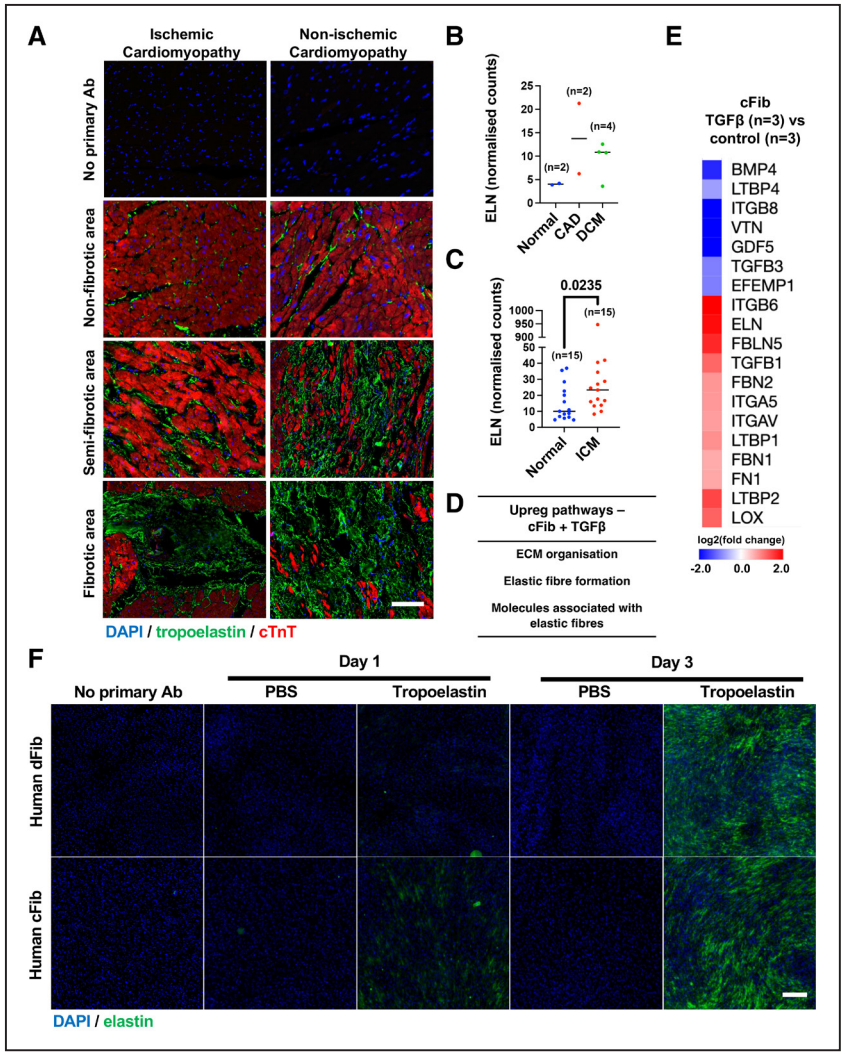

Figure 6. Tropoelastin is increased in ischemic human heart disease and in human cardiac fibroblast (cFib) differentiation or tropoelastin treatment.

A, Immunohistochemical (IHC) staining for human tropoelastin (green) and cardiomyocyte marker, cardiac troponin T (cTnT, red), samples were from ischemic and nonischemic cardiomyopathy patient cardiac tissue, images taken from fibrotic and nonfibrotic regions of interest. Scale bar=100 µm. **B** and **C**, Tropoelastin gene (*ELN*) expression from publicly available single-cell (**B**) and bulk (**C**) RNA sequencing (RNAseq) cardiac tissue datasets, coronary artery disease (CAD; n=2), dilated cardiomyopathy (DCM; n=4), schemic cardiomyopathy (ICM; n=15), (**C**) was statistically analyzed using Mann-Whitney test with exact *P*-value represented to 4 decimal points. **D**, Selected statistically significant upregulated Reactome pathways in cFib treated with transforming growth factor β (TGFβ). **E**, Heatmap of statistically significantly down/upregulated Reactome elastin fiber formation curated genes in cFib treated with TGFβ, as compared to untreated controls. **F**, Immunocytochemistry images of cFib cultured for 7 days, treated with tropoelastin/PBS for 1 or 3 days and stained for elastin (green). Scale bar=100 µm. Ab indicates antibody and DAPI, 4′,6-diamidino-2-phenylindole.

Tropoelastin is Increased in Human Heart Disease and in Human Cardiac Myofibroblasts

To assess whether tropoelastin is increased in human cardiac fibrosis, we used immunohistochemical to probe tropoelastin protein expression in human ischemic and nonischemic-dilated cardiomyopathy samples (Figure 6A; Figure S15). We showed increased elastin expression in scar versus remote areas in both disease types (Figure 6A; Figure S15). To analyze *ELN* expression in similar settings, we analyzed publicly available RNAseq datasets (Figure 6B and 6C). These data showed increased *ELN* in ischemic cardiomyopathy and coronary artery disease (Figure 6B and 6C). Taken together, these results show tropoelastin is increased in areas of replacement fibrosis in human heart disease.

We next determined whether cFibs synthesize elastin during myofibroblast differentiation, an integral process in the latter stages of post-MI scar remodeling. Three primary cFib lines derived from cardiac tissue explants were treated with transforming growth factor-beta to induce myofibroblast differentiation and compared to untreated controls using RNAseq. Reactome pathway analysis looking at upregulated genes showed that Elastic fiber formation and Molecules associated with elastic fibers were amongst the statistically significant upregulated pathways (Figure 6D). Using the curated gene set Elastic fiber formation, we generated a heatmap showing the significantly upregulated elastin-related genes (Figure 6E). Notably upregulated genes in the list essential[35] for elastogenesis include *ELN*, fibronectin-1 (*FN1*), fibulin-5 (*FBLN5*), fibrillin-1 and -2 (*FBN1*, *FBN2*), integrin subunit alpha-5 and -V (*ITGA5*, *ITGAV*), latent binding protein-1 and -2 (*LTBP1*, *LTBP2*), and lysyl oxidase (*LOX*; Figure 6E). We therefore demonstrated that human cFib increase elastin fiber synthesis following myofibroblast differentiation; an integral process that occurs during post-MI scar formation.

Finally, we determined whether elastogenesis in cFib could be increased with tropoelastin treatment. This aimed to test the hypothesis that cFib can increase elastin synthesis, which could be therapeutically used to increase elastin after post-MI tropoelastin delivery in a patient. After 1 day, elastin fibers were observed in

tropoelastin samples but not PBS controls (Figure 6F). By day 3, a substantial layer of elastin fibers was present, comparable to human primary dermal fibroblast positive controls, in contrast to no visible fibers in the PBS controls (Figure 6F). These data demonstrate the ability of human cFib to synthesize elastin after tropoelastin treatment.

DISCUSSION

Following MI, necrotic cardiomyocytes are replaced by a stiff collagen I-rich fibrotic scar, leading to impaired heart function.[2] Tropoelastin, the subunit of elastin, has a much lower stiffness than collagen I,[11,12] and has previously shown efficacy in wound healing applications.[20,21] To date, no study has investigated the therapeutic use of purified human tropoelastin to alter scar formation, nor has any study elucidated the relevance of tropoelastin in human heart disease. Our study reveals that by increasing scar elastogenesis, tropoelastin reduces scar expansion and significantly improves heart function, thus demonstrating tropoelastin can be an efficacious post-MI treatment when delivered in the early subacute stage. We also reveal for the first time increased elastogenesis in human MI scar formation and during human cFib-myofibroblast differentiation. The rigorous assessment in this study therefore increases our understanding of tropoelastin in cardiac wound healing and of elastogenesis post-MI. Furthermore, our data make a compelling case for tropoelastin translation as a post-MI therapeutic to decrease morbidity and mortality in a subacute setting.

Rodent post-MI therapeutics are traditionally administered via systemic tail vein injection,[36] osmotic minipump insertion,[37] or direct myocardial injections.[38] Limitations of these methods include limited cardiac targeting, painful thoracotomy surgery with increased mortality, and therapeutic delivery limited to the time of MI surgery. Our ultrasound-guided intramyocardial therapeutic delivery method (Figure 1) provides a less invasive and simpler method to gain access to the myocardium, with a 0% mortality rate following procedure. It also allows direct cardiac access at a timepoint of a researcher's choosing with improved animal welfare.

Two notable studies have previously investigated the effects of increasing elastin post-MI.[22,23] Both used cell lines transfected with the rat tropoelastin gene and injected into the hearts using a rat MI model.[22,23] In support of our results, both studies showed reduced scar expansion and improved heart function. However, a critical distinction is the use of transduced rat cells as a rat elastin delivery vehicle in these prior studies, rather than the purified human tropoelastin in our study. Paracrine cell signaling from transplanted cells could have confounded previous results, whereas our study avoided these effects and provided evidence that tropoelastin itself is responsible for improved function. Additionally, unlike cell-derived equivalents, tropoelastin is a natural biomaterial that has been clinically tested for dermal applications and is an attractive post-MI therapeutic with the potential for accelerated clinical translation. Our targeted injection protocol also provides control over the dosage and concentration of therapeutic administration into the myocardium, thus establishing a superior route of delivery for future studies.

The post-MI scar is primarily composed of stiff collagen I with an absence of viable contractile cardiomyocytes.[2] This reduction in functional myocardium contributes to reduced heart function. Some post-MI therapeutics improve heart function by reducing scar size and thereby increasing the quantity of viable myocardium.[39–42] In our study, we show tropoelastin significantly reduces scar size (Figure 4A through 4C) and could be responsible for most of the functional improvements observed. However, an understanding into the exact mechanism behind tropoelastin ability to prevent scar expansion is not yet known.

As tropoelastin and elastin have relatively low (~3 kPa and ~1 MPa) elastic moduli, compared to collagen (~160–7500 MPa),[11,12] it can be reasonably assumed that increasing their proportion within the scar would alter its mechanical properties. Previous studies have shown cardiac compliance and stiffness are major driving factors that alter cardiac function in diseased hearts.[5–7,43,44] Therefore, our study suggests that the beneficial effects of tropoelastin are potentially due to modification of scar mechanical properties. To this end, our ex vivo mechanical testing of IZ tissue (Figure S13) demonstrated similar elastic moduli between sham, healthy and MI+Tropo groups. In contrast, MI+PBS controls showed an expected increase in IZ stiffness. This may suggest that tropoelastin improves heart function by reducing infarct scar stiffness. Notably, further studies would require increased animal numbers and other modes of mechanical testing to fully characterize the infarct material properties.

Other groups have also targeted LV scar mechanics by injecting naturally derived extracellular components into MI models.[24–27] Of significance, Diaz et al[25] have shown in a long-term post-MI study (13.5 weeks) that injecting a myocardial-derived ECM hydrogel improved heart function, increased LV wall thickening, and reduced fibrosis. This injectable matrix technology has also been used in early clinical trials.[27] In our subacute post-MI study, we also show improved heart function (Figure 2), increased LVAW systolic thickness (Figure 2), and reduced fibrosis (Figure 4C). Therefore, in light of previous studies and their clinical translation, our findings are encouraging for the potential future clinical translation of tropoelastin as a post-MI therapeutic.

Elastogenesis is prominent in early development but minimal in the adult body except in some cases of injury

and disease.[11,14–19] In the post-MI rodent setting, the literature is split on the significance of elastogenesis. Mizuno et al[23] showed no post-MI elastin deposition, while Yu et al[45] showed decreased elastin in untreated infarcted rats. A second study by Mizuno et al[22] and other more rigorous studies utilizing MRI combined with histological techniques[17–19] shows increased elastin deposition in infarcted tissue.[22] These latter studies support our findings that elastogenesis is increased in both tropoelastin treated and vehicle control infarcts. Our data (Figures 4D through 4H and 6A through 6E; Figure S15) demonstrate that elastogenesis has an underappreciated role in rat and human cardiac fibrosis. Importantly, our study also shows that therapeutic delivery of exogenous tropoelastin can stabilize the postinfarct scar through increased elastogenesis but has no effect in the uninjured heart (Figure 4). We therefore provide insight into the integral role of elastogenesis during post-MI LV remodeling and demonstrate that manipulation of this process can improve cardiac function.

In our study, we saw increased scar elastogenesis in tropoelastin-treated rats (Figure 4D through 4H). Elastogenesis requires a number of phases: tropoelastin synthesis, coacervation, deposition, and cross-linking.[11] Therapeutically, we provided purified tropoelastin, aiming for the second phase of coacervation to occur in vivo. This requires temperatures above 37°C and a concentration of >1 mg/mL.[11,46,47] However, the presence of glycosaminoglycans, such as heparan sulfate, abolishes this critical concentration to an undetectable value.[47] It is also known that heparan sulfate not only exists in the uninjured heart but also in upregulated post-MI.[48] Therefore, once injected into the heart, our 1 mg/mL solution would have reached ≈37°C[49] and likely interacted with heparan sulfate. Subsequently, it can be reasonably assumed that tropoelastin coacervated upon injection and was capable of microassembly. Our rat RNAseq data revealed that the increased elastogenesis observed in tropoelastin-treated infarcted rats likely occurred <11 days post-MI (<7 days treatment; Figure 5). This is not an indication that elastogenesis had ceased, but rather that any additional tropoelastin-induced elastogenesis was no longer detectable. For complete elastogenesis, cross-linking by LOX or lysyl oxidase-like enzymes is required. These enzymes are synthesized predominantly by fibroblasts/myofibroblasts in the post-MI scar.[50] In our study, we observed increased LOX expression in cFib-myofibroblast differentiation (Figure 6E). We also show tropoelastin-treated cFib synthesize increased elastin (Figure 6F). Taken together, these results suggest injected tropoelastin underwent elastogenesis by forming a coacervate and LOX/lysyl oxidase-like cross-linking by cardiac fibroblasts/myofibroblasts. Additionally, our evidence in primary human cell lines (Figure 6) suggests a similar process could occur if tropoelastin therapy were to progress to human clinical trials.

A complex immune response is required for post-MI scar formation.[2] Many post-MI therapeutics have been developed that target this immune response in an attempt to prevent excessive remodeling and scar expansion.[51–53] Our rat RNAseq data showed that tropoelastin downregulates gene expression within multiple immune response-related pathways. Similarly, previous studies have also shown that tropoelastin can modulate the immune system, having both pro-inflammatory and anti-inflammatory effects in different settings.[54,55] Our data therefore suggests that tropoelastin may not only improve heart function by improving scar mechanical properties but may also interact with the immune system to prevent excessive remodeling. However, complex immune cell profiling using high-dimensional platforms, such as imaging mass cytometry, are required for future studies to elucidate a deeper understanding into the immune response.

A robust method of synthesizing tropoelastin in vitro[56] has enabled the development of a wide range of clinical applications.[57] This includes applications enhancing cutaneous wound healing,[20,21] which draws multiple parallels with the post-MI healing setting.[58] Our study adds to this growing list of potential applications[20,21,57,59] and buttresses the notion that cutaneous and ischemic injury share some common mechanisms.

Patients with delayed presentation of ST-elevation MI present a decreased likelihood of achieving myocardial salvage via reperfusion.[60] These substantial number of patients have a poorer prognosis and can result from a range of factors such as ST-elevation MI occurring an increased distance from hospital or unrecognized symptoms.[60,61] As this study focuses on tropoelastin in a subacute setting, we propose its clinical relevance as an early post-MI therapeutic to treat patients presenting with completed ST-elevation MI (indicated by presence of Q waves on electrocardiogram). In this regard and through its effects in modulating post-MI remodeling, tropoelastin therefore bears some similarity to drugs historically used as subacute therapeutics, such as angiotensin converting enzyme inhibitors.[62] Following the subacute effects of MI and during progressive heart failure, the heart undergoes compensatory LV dilatation.[63] Therefore, to understand the effects of tropoelastin in a more chronic setting, future studies will likely concentrate on injecting tropoelastin 2 to 3 weeks post-MI with longer term (≥6 months) functional studies to elucidate its effects on LV dilatation. Other future studies may focus on the application of tropoelastin in a large animal preclinical model and could serve as the next step toward clinical translation.

In conclusion, we demonstrate for the first time that purified human tropoelastin significantly improves cardiac function in a rodent model of MI by reducing deleterious cardiac remodeling. We also show that elastogenesis is an integral post-MI process in both humans and rats and can be manipulated for beneficial cardiac outcomes. With

therapeutic tropoelastin already clinically available, tropoelastin could see accelerated bench-to-bedside application and improve the lives of millions of heart failure patients worldwide.

ARTICLE INFORMATION

Received March 28, 2022; revision received November 15, 2022; accepted November 22, 2022.

Affiliations

Centre for Heart Research, Westmead Institute for Medical Research, NSW, Australia (R.D.H., S.K., T.D., S.C., F.N.R., J.L., Z.E.C., E.K., J.J.H.C.). Department of Cardiology, Westmead Hospital, NSW, Australia (T.D., J.L., E.K., P.B., L.T., J.J.H.C.). Sydney Medical School, University of Sydney, NSW, Australia (R.D.H., T.D., F.R., Z.E.C., E.K., J.J.H.C.).Charles Perkins Centre, University of Sydney, NSW, Australia (S.M.M., A.S.W.). School of Life and Environmental Sciences, University of Sydney, NSW, Australia (S.M.M., A.S.W.). School of Biomedical Engineering, University of Sydney, NSW, Australia (I.R.). School of Chemistry, University of New South Wales, Australia (I.R.). Centre for Cancer Research, Westmead Institute for Medical Research, NSW, Australia (T.D., D.G.). Westmead Breast Cancer Institute, NSW, Australia (D.G.). Westmead Clinical School, University of Sydney, NSW, Australia (D.G., L.T.). Heart Research Institute, Sydney, NSW, Australia (E.S.). Department of Medicine, Division of Cardiology, University of Washington School of Medicine, Seattle, WA (A.S.S.-O.). Sydney Nano, University of Sydney, NSW, Australia (A.S.W.).

Acknowledgments

We acknowledge Professor Damien Harkin from the Queensland University of Technology for his modified Verhoeff van Gieson staining protocol. We acknowledge the Charles Perkins Centre Preclinical Facilities team (Sydney Imaging) for their assistance in echocardiography. Special thanks to Sofie Trajanovska and Nana Sunn who previously worked in the preclinical facility. Image acquisition and analysis were performed at Westmead Imaging Facility, which is supported by the Westmead Institute for Medical Research and the National Health and Medical Research Council.

Sources of Funding

This study was funded by the Heart Foundation Vanguard Grant Award 103055. J. Chong was supported by an Investigator Grant APP1194139 from National Health and Medical Research Council of Australia and a Clinician Researcher grant from the Ministry of Health, New South Wales. A. Weiss was supported by an Investigator Grant (APP1195827) from the National Health and Medical Research Council of Australia.

Disclosures

A. Weiss is the Scientific Founder of Elastagen Pty Ltd, which was sold to Allergan, an AbbVie company. The other authors report no conflicts.

Supplemental Material

Supplemental Methods
Figures S1–S15
Videos S1–S16
References 64–69

REFERENCES

1. Virani SS, Alonso A, Benjamin EJ, Bittencourt MS, Callaway CW, Carson AP, Chamberlain AM, Chang AR, Cheng S, Delling FN, et al. Heart disease and stroke statistics-2020 update: a report from the American Heart Association. *Circulation.* 2020;141:E139–E596. doi: 10.1161/CIR.0000000000000757
2. Hume RD, Chong JJH. The cardiac injury immune response as a target for regenerative and cellular therapies. *Clin Ther.* 2020;42:1923–1943. doi: 10.1016/j.clinthera.2020.09.006
3. Hiesinger W, Brukman MJ, McCormick RC, Fitzpatrick JR, Frederick JR, Yang EC, Muenzer JR, Marotta NA, Berry MF, Atluri P, et al. Myocardial tissue elastic properties determined by atomic force microscopy after stromal cell-derived factor 1α angiogenic therapy for acute myocardial infarction in a murine model. *J Thorac Cardiovasc Surg.* 2012;143:962–966. doi: 10.1016/j.jtcvs.2011.12.028
4. Rusu M, Hilse K, Schuh A, Martin L, Slabu I, Stoppe C, Liehn EA. Biomechanical assessment of remote and postinfarction scar remodeling following myocardial infarction. *Sci Rep.* 2019;9:16744. doi: 10.1038/s41598-019-53351-7
5. Clarke SA, Richardson WJ, Holmes JW. Modifying the mechanics of healing infarcts: is better the enemy of good?. *J Mol Cell Cardiol.* 2016;93:115–124. doi: 10.1016/j.yjmcc.2015.11.028
6. Leong CO, Leong CN, Abed AA, Ahmad Bakir A, Liew YM, Dokos S, Lim E. Computational modelling of the effect of infarct stiffness on regional myocardial mechanics. *Annu Int Conf IEEE Eng Med Biol Soc IEEE Eng Med Biol Soc Annu Int Conf.* 2019;2019:6952–6955. doi: 10.1109/EMBC.2019.8856771
7. Richardson WJ, Clarke SA, Alexander Quinn T, Holmes JW. Physiological implications of myocardial scar structure. *Compr Physiol.* 2015;5:1877–1909. doi: 10.1002/cphy.c140067
8. Khalil NN, McCain ML. Engineering the cellular microenvironment of post-infarct myocardium on a chip. *Front Cardiovasc Med* 2021;8:709871. doi: 10.3389/fcvm.2021.709871
9. Rouillard AD, Holmes JW. Coupled agent-based and finite-element models for predicting scar structure following myocardial infarction. *Prog Biophys Mol Biol.* 2014;115:235–243. doi: 10.1016/j.pbiomolbio.2014.06.010
10. Baldock C, Oberhauser AF, Ma L, Lammie D, Siegler V, Mithieux SM, Tu Y, Chow JYH, Suleman F, Malfois M, et al. Shape of tropoelastin, the highly extensible protein that controls human tissue elasticity. *Proc Natl Acad Sci USA.* 2011;108:4322–4327. doi: 10.1073/pnas.1014280108
11. Ozsvar J, Yang C, Cain SA, Baldock C, Tarakanova A, Weiss AS. Tropoelastin and Elastin Assembly. *Front Bioeng Biotechnol.* 2021;9:643110. doi: 10.3389/fbioe.2021.643110
12. Guthold M, Liu W, Sparks EA, Jawerth LM, Peng L, Falvo M, Superfine R, Hantgan RR, Lord ST. A comparison of the mechanical and structural properties of fibrin fibers with other protein fibers. *Cell Biochem Biophys.* 2007;49:165–181. doi: 10.1007/s12013-007-9001-4
13. Wagenseil JE, Mecham RP. Elastin in large artery stiffness and hypertension. *J Cardiovasc Transl Res.* 2012;5:264–273. doi: 10.1007/s12265-012-9349-8
14. Duca L, Blaise S, Romier B, Laffargue M, Gayral S, El Btaouri H, Kawecki C, Guillot A, Martiny L, Debelle L, et al. Matrix ageing and vascular impacts: focus on elastin fragmentation. *Cardiovasc Res.* 2016;110:298–308. doi: 10.1093/cvr/cvw061
15. Phinikaridou A, Lacerda S, Lavin B, Andia ME, Smith A, Saha P, Botnar RM. Tropoelastin: a novel marker for plaque progression and instability. *Circ Cardiovasc Imaging.* 2018;11:e007303. doi: 10.1161/CIRCIMAGING.117.007303
16. Parks WC, Roby JD, Wu LC, Gross LE. Cellular expression of tropoelastin mRNA splice variants. *Matrix.* 1992;12:156–162. doi: 10.1016/s0934-8832(11)80057-0
17. Elkenhans B, Protti A, Shah A, Onthank D, Botnar R. Visualization of elastin using cardiac magnetic resonance imaging after myocardial infarction as inflammatory response. *Sci Rep.* 2021;11:11004. doi: 10.1038/s41598-021-90092-y
18. Protti A, Lavin B, Dong X, Lorrio S, Robinson S, Onthank D, Shah AM, Botnar RM. Assessment of myocardial remodeling using an elastin/tropoelastin specific agent with high field magnetic resonance imaging (MRI). *J Am Heart Assoc.* 2015;4:e001851. doi: 10.1161/JAHA.115.001851
19. Wildgruber M, Bielicki I, Aichler M, Kosanke K, Feuchtinger A, Settles M, Onthank DC, Cesati RR, Robinson SP, Huber AM, et al. Assessment of myocardial infarction and postinfarction scar remodeling with an elastin-specific magnetic resonance agent. *Circ Cardiovasc Imaging.* 2014;7:321–329. doi: 10.1161/CIRCIMAGING.113.001270
20. Wang Y, Mithieux SM, Kong Y, Wang XQ, Chong C, Fathi A, Dehghani F, Panas E, Kemnitzer J, Daniels R, et al. Tropoelastin incorporation into a dermal regeneration template promotes wound angiogenesis. *Adv Healthc Mater.* 2015;4:577–584. doi: 10.1002/adhm.201400571
21. Mithieux SM, Aghaei-Ghareh-Bolagh B, Yan L, Kuppan KV, Wang Y, Garces-Suarez F, Li Z, Maitz PK, Carter EA, Limantoro C, et al. Tropoelastin implants that accelerate wound repair. *Adv Healthc Mater.* 2018;7:1701206. doi: 10.1002/adhm.201701206
22. Mizuno T, Yau TM, Weisel RD, Kiani CG, Li R-K. Elastin stabilizes an infarct and preserves ventricular function. *Circulation.* 2005;112:I81–I88. doi: 10.1161/01.CIRCULATIONAHA.105.523795
23. Mizuno T, Mickle DAG, Kiani CG, Li RK. Overexpression of elastin fragments in infarcted myocardium attenuates scar expansion and heart dysfunction. *Am J Physiol Heart Circ Physiol.* 2005;288: H2819–H2827. doi: 10.1152/ajpheart.00862.2004

24. Singelyn JM, DeQuach JA, Seif-Naraghi SB, Littlefield RB, Schup-Magoffin PJ, Christman KL. Naturally derived myocardial matrix as an injectable scaffold for cardiac tissue engineering. *Biomaterials.* 2009;30:5409–5416. doi: 10.1016/j.biomaterials.2009.06.045
25. Diaz MD, Tran E, Spang M, Wang R, Gaetani R, Luo CG, Braden R, Hill RC, Hansen KC, DeMaria AN, et al. Injectable myocardial matrix hydrogel mitigates negative left ventricular remodeling in a chronic myocardial infarction model. *JACC Basic to Transl Sci.* 2021;6:350. doi: 10.1016/j.jacbts.2021.01.003
26. Curley CJ, Dolan EB, Otten M, Hinderer S, Duffy GP, Murphy BP. An injectable alginate/extra cellular matrix (ECM) hydrogel towards acellular treatment of heart failure. *Drug Deliv Transl Res.* 2019;9:1–13. doi: 10.1007/s13346-018-00601-2
27. Traverse JH, Henry TD, Dib N, Patel AN, Pepine C, Schaer GL, DeQuach JA, Kinsey AM, Chamberlin P, Christman KL. First-in-man study of a cardiac extracellular matrix hydrogel in early and late myocardial infarction patients. *JACC Basic to Transl Sci.* 2019;4:659–669. doi: 10.1016/j.jacbts.2019.07.012
28. Fomovsky GM, Thomopoulos S, Holmes JW. Contribution of extracellular matrix to the mechanical properties of the heart. *J Mol Cell Cardiol.* 2010;48:490–496. doi: 10.1016/j.yjmcc.2009.08.003
29. Ma Y, Yabluchanskiy A, Lindsey ML. Neutrophil roles in left ventricular remodeling following myocardial infarction. *Fibrogenesis Tissue Repair.* 2013;6:11. doi: 10.1186/1755-1536-6-11
30. Appadurai V, D'Elia N, Mew T, Tomlinson S, Chan J, Hamilton-Craig C, Scalia GM. Global longitudinal strain as a prognostic marker in cardiac resynchronisation therapy: a systematic review. *Int J Cardiol Hear Vasc.* 2021;35:100849. doi: 10.1016/j.ijcha.2021.100849
31. Polacin M, Karolyi M, Eberhard M, Gotschy A, Baessler B, Alkadhi H, Kozerke S, Manka R. Segmental strain analysis for the detection of chronic ischemic scars in non-contrast cardiac MRI cine images. *Sci Rep.* 2021;11:12376. doi: 10.1038/s41598-021-90283-7
32. Bleeker GB, Bax JJ, Steendijk P, Schalij MJ, van der Wall EE. Left ventricular dyssynchrony in patients with heart failure: pathophysiology, diagnosis and treatment. *Nat Clin Pract Cardiovasc Med.* 2006;3:213–219. doi: 10.1038/ncpcardio0505
33. Fudim M, Fathallah M, Shaw LK, Liu PR, James O, Samad Z, Piccini JP, Hess PL, Borges-Neto S. The prognostic value of diastolic and systolic mechanical left ventricular dyssynchrony among patients with coronary heart disease. *JACC Cardiovasc Imaging.* 2019;12:1215–1226. doi: 10.1016/j.jcmg.2018.05.018
34. Palazzuoli A, Beltrami M, Gennari L, Dastidar AG, Nuti R, McAlindon E, Angelini GD, Bucciarelli-Ducci C. The impact of infarct size on regional and global left ventricular systolic function: a cardiac magnetic resonance imaging study. *Int J Cardiovasc Imaging.* 2015;31:1037–1044. doi: 10.1007/s10554-015-0657-3
35. Godwin ARF, Singh M, Lockhart-Cairns MP, Alanazi YF, Cain SA, Baldock C. The role of fibrillin and microfibril binding proteins in elastin and elastic fibre assembly. *Matrix Biol.* 2019;84:17–30. doi: 10.1016/j.matbio.2019.06.006
36. Rashid FN, Clayton ZE, Ogawa M, Perdomo J, Hume RD, Kizana E, Chong JJH. Platelet derived growth factor-A (Pdgf-a) gene transfer modulates scar composition and improves left ventricular function after myocardial infarction. *Int J Cardiol.* 2021;341:24–30. doi: 10.1016/j.ijcard.2021.07.021
37. Asli NS, Xaymardan M, Forte E, Waardenberg AJ, Cornwell J, Janbandhu V, Kesteven S, Chandrakanthan V, Malinowska H, Reinhard H, et al. PDGFRα signaling in cardiac stem and stromal cells modulates quiescence, metabolism and self-renewal, and promotes anatomical and functional repair. *bioRxiv.* Preprint posted online June 13, 2019. doi: 10.1101/225979
38. Virag JAI, Lust RM. Coronary artery ligation and intramyocardial injection in a murine model of infarction. *J Vis Exp.* 2011;(52):2581. doi: 10.3791/2581
39. Garbayo E, Gavira JJ, De Yebenes MG, Pelacho B, Abizanda G, Lana H, Blanco-Prieto MJ, Prosper F. Catheter-based intramyocardial injection of FGF1 or NRG1-loaded MPs improves cardiac function in a preclinical model of ischemia-reperfusion. *Sci Rep.* 2016;6:25932. doi: 10.1038/srep25932
40. Macarthur JW, Purcell BP, Shudo Y, Cohen JE, Fairman A, Trubelja A, Patel J, Hsiao P, Yang E, Lloyd K, et al. Sustained release of engineered stromal cell-derived factor 1-α from injectable hydrogels effectively recruits endothelial progenitor cells and preserves ventricular function after myocardial infarction. *Circulation.* 2013;128: S79–S86. doi: 10.1161/CIRCULATIONAHA.112.000343
41. Ruvinov E, Leor J, Cohen S. The promotion of myocardial repair by the sequential delivery of IGF-1 and HGF from an injectable alginate biomaterial in a model of acute myocardial infarction. *Biomaterials.* 2011;32:565–578. doi: 10.1016/j.biomaterials.2010.08.097
42. Bassat E, Mutlak YE, Genzelinakh A, Shadrin IY, Baruch Umansky K, Yifa O, Kain D, Rajchman D, Leach J, Riabov Bassat D, et al. The extracellular matrix protein agrin promotes heart regeneration in mice. *Nature.* 2017;547:179–184. doi: 10.1038/nature22978
43. Zile MR, Baicu CF, Ikonomidis JS, Stroud RE, Nietert PJ, Bradshaw AD, Slater R, Palmer BM, Van Buren P, Meyer M, et al. Myocardial stiffness in patients with heart failure and a preserved ejection fraction: contributions of collagen and titin. *Circulation.* 2015;131:1247–1259. doi: 10.1161/CIRCULATIONAHA.114.013215
44. Caporizzo MA, Prosser BL. Need for speed: the importance of physiological strain rates in determining myocardial stiffness. *Front Physiol.* 2021;12:696694. doi: 10.3389/fphys.2021.696694
45. Yu Y, Yin G, Bao S, Guo Z. Kinetic alterations of collagen and elastic fibres and their association with cardiac function in acute myocardial infarction. *Mol Med Rep.* 2018;17:3519–3526. doi: 10.3892/mmr.2017.8347
46. Toonkool P, Jensen SA, Maxwell AL, Weiss AS. hydrophobic domains of human tropoelastin interact in a context-dependent manner. *J Biol Chem.* 2001;276:44575–44580. doi: 10.1074/jbc.M107920200
47. Tu Y, Weiss AS. Glycosaminoglycan-mediated coacervation of tropoelastin abolishes the critical concentration, accelerates coacervate formation, and facilitates spherule fusion: implications for tropoelastin microassembly. *Biomacromolecules.* 2008;9:1739–1744. doi: 10.1021/bm7013153
48. Korf-Klingebiel M, Reboll MR, Grote K, Schleiner H, Wang Y, Wu X, Klede S, Mikhed Y, Bauersachs J, Klintschar M, et al. Heparan sulfate-editing extracellular sulfatases enhance VEGF bioavailability for ischemic heart repair. *Circ Res.* 2019;125:787–801. doi: 10.1161/CIRCRESAHA.119.315023
49. Lillie LE, Temple NJ, Florence LZ. Reference values for young normal Sprague-Dawley rats: weight gain, hematology and clinical chemistry. *Hum Exp Toxicol.* 1996;15:612–616. doi: 10.1177/096032719601500802
50. González-Santamaría J, Villalba M, Busnadiego O, López-Olañeta MM, Sandoval P, Snabel J, López-Cabrera M, Erler JT, Hanemaaijer R, Lara-Pezzi E, et al. Matrix cross-linking lysyl oxidases are induced in response to myocardial infarction and promote cardiac dysfunction. *Cardiovasc Res.* 2016;109:67–78. doi: 10.1093/cvr/cvv214
51. Buckley LF, Abbate A. Interleukin-1 blockade in cardiovascular diseases: from bench to bedside. *BioDrugs.* 2018;32:111–118. doi: 10.1007/s40259-018-0274-5
52. Kim Y, Nurakhayev S, Nurkesh A, Zharkinbekov Z, Saparov A. Macrophage polarization in cardiac tissue repair following myocardial infarction. *Int J Mol Sci.* 2021;22:2715. doi: 10.3390/ijms22052715
53. Jing R, Long TY, Pan W, Li F, Xie QY. IL-6 knockout ameliorates myocardial remodeling after myocardial infarction by regulating activation of M2 macrophages and fibroblast cells. *Eur Rev Med Pharmacol Sci.* 2019;23:6283–6291. doi: 10.26355/eurrev_201907_18450
54. Almine JF, Wise SG, Hiob M, Singh NK, Tiwari KK, Vali S, Abbasi T, Weiss AS. Elastin sequences trigger transient proinflammatory responses by human dermal fibroblasts. *FASEB J.* 2013;27:3455–3465. doi: 10.1096/fj.13-231787
55. Liu H, Wise SG, Rnjak-Kovacina J, Kaplan DL, Bilek MMM, Weiss AS, Fei J, Bao S. Biocompatibility of silk-tropoelastin protein polymers. *Biomaterials.* 2014;35:5138–5147. doi: 10.1016/j.biomaterials.2014.03.024
56. Martin SL, Vrhovski B, Weiss AS. Total synthesis and expression in Escherichia coli of a gene encoding human tropoelastin. *Gene.* 1995;154:159–166. doi: 10.1016/0378-1119(94)00848-m
57. Wise SG, Yeo GC, Hiob MA, Rnjak-Kovacina J, Kaplan DL, Ng MKC, Weiss AS. Tropoelastin: a versatile, bioactive assembly module. *Acta Biomater.* 2014;10:1532–1541. doi: 10.1016/j.actbio.2013.08.003
58. Richardson RJ. Parallels between vertebrate cardiac and cutaneous wound healing and regeneration. *NPJ Regen Med.* 2018;3:21. doi: 10.1038/s41536-018-0059-y
59. Xie H, Lucchesi L, Zheng B, Ladich E, Pineda T, Merten R, Gregory C, Rutten M, Gregory K. Treatment of burn and surgical wounds with recombinant human tropoelastin produces new elastin fibers in scars. *J Burn Care Res.* 2017;38:e859–e867. doi: 10.1097/BCR.0000000000000507
60. Devon HA, Mirzaei S, Zègre-Hemsey J. Typical and atypical symptoms of acute coronary syndrome: time to retire the terms?. *J Am Heart Assoc.* 2020;9: e015539. doi: 10.1161/JAHA.119.015539 [Internet]
61. Postma S, Dambrink JHE, de Boer MJ, Gosselink ATM, Ottervanger JP, Koopmans PC, ten Berg JM, Suryapranata H, van't Hof AWJ. The influence of residential distance on time to treatment in ST-elevation myocardial

infarction patients. *Netherlands Hear J.* 2014;22:513. doi: 10.1007/s12471-014-0599-8
62. Sim HW, Zheng H, Richards AM, Chen RW, Sahlen A, Yeo KK, Tan JW, Chua T, Tan HC, Yeo TC, et al. Beta-blockers and renin-angiotensin system inhibitors in acute myocardial infarction managed with inhospital coronary revascularization. *Sci Rep.* 2020;10:15184. doi: 10.1038/s41598-020-72232-y
63. Gaudron P, Eilles C, Ertl G, Kochsiek K. Compensatory and noncompensatory left ventricular dilatation after myocardial infarction: time course and hemodynamic consequences at rest and during exercise. *Am Heart J.* 1992;123:377–385. doi: 10.1016/0002-8703(92)90649-g
64. Verhoeff FH. Some new staining methods of wide applicability; including a rapid differential stain for elastic tissue. *J Am Assoc.* 1908;50:876–877 doi: 10.1001/jama.1908.25310370042004a.
65. Schindelin J, Arganda-Carreras I, Frise E, Kaynig V, Longair M, Pietzsch T, Preibisch S, Rueden C, Saalfeld S, Schmid B, et al. Fiji: an open-source platform for biological-image analysis. *Nat Methods.* 2012;9:676–682. doi: 10.1038/nmeth.2019
66. McQuin C, Goodman A, Chernyshev V, Kamentsky L, Cimini BA, Karhohs KW, Doan M, Ding L, Rafelski SM, Thirstrup D, et al. CellProfiler 3.0: Next-generation image processing for biology. *PLoS Biol.* 2018;16:e2005970. doi: 10.1371/journal.pbio.2005970
67. Mahi NA, Najafabadi MF, Pilarczyk M, Kouril M, Medvedovic M. GREIN: an interactive web platform for re-analyzing GEO rna-seq data. *Sci Rep.* 2019;9:7580. doi: 10.1038/s41598-019-43935-8
68. Wang L, Yu P, Zhou B, Song J, Li Z, Zhang M, Guo G, Wang Y, Chen X, Han L, et al. Single-cell reconstruction of the adult human heart during heart failure and recovery reveals the cellular landscape underlying cardiac function. *Nat Cell Biol.* 2020;22:108–119. doi: 10.1038/s41556-019-0446-7
69. Mithieux SM, Weiss AS. Design of an elastin-layered dermal regeneration template. *Acta Biomater.* 2017;52:33–40. doi: 10.1016/j.actbio.2016.11.054